

Published in final edited form as:

Br J Ophthalmol. 2008 May ; 92(5): 705–711. doi:10.1136/bjo.2007.133587.

Intravitreal properties of porous silicon photonic crystals:

a potential self-reporting intraocular drug-delivery vehicle

L Cheng¹, E Anglin², F Cunin³, D Kim², M J Sailor², I Falkenstein¹, A Tammewar¹, and W R Freeman¹

¹Jacobs Retina Center at Shiley Eye Center, UCSD, La Jolla, CA, USA

²Department of Chemistry and Biochemistry, UCSD, La Jolla, CA, USA

³Laboratoire de Matériaux Catalytiques et Catalyse en Chimie Organique, UMR5618 ENSCM-CNRS-UMI, Institut Gerhardt, Montpellier, France

Abstract

Aim—To determine the suitability of porous silicon photonic crystals for intraocular drug-delivery.

Methods—A rugate structure was electrochemically etched into a highly doped p-type silicon substrate to create a porous silicon film that was subsequently removed and ultrasonically fractured into particles. To stabilise the particles in aqueous media, the silicon particles were modified by surface alkylation (using thermal hydrosilylation) or by thermal oxidation. Unmodified particles, hydrosilylated particles and oxidised particles were injected into rabbit vitreous. The stability and toxicity of each type of particle were studied by indirect ophthalmoscopy, biomicroscopy, tonometry, electroretinography (ERG) and histology.

Results—No toxicity was observed with any type of the particles during a period of >4 months. Surface alkylation led to dramatically increased intravitreal stability and slow degradation. The estimated vitreous half-life increased from 1 week (fresh particles) to 5 weeks (oxidised particles) and to 16 weeks (hydrosilylated particles).

Conclusion—The porous silicon photonic crystals showed good biocompatibility and may be used as an intraocular drug-delivery system. The intravitreal injectable porous silicon photonic crystals may be engineered to host a variety of therapeutics and achieve controlled drug release over long periods of time to treat chronic vitreoretinal diseases.

There is an important medical need for a minimally invasive, controllable and monitorable drug-delivery system that would enable long-acting local treatment of intraocular diseases affecting the retina and choroid. In particular, diseases such as choroidal neovascularisation (CNV) in age-related macular degeneration (ARMD), proliferative vitreoretinopathy (PVR) associated with retinal detachment and trauma, and refractory uveitis would benefit greatly. For those chronic refractory diseases, drug delivery to the vitreous, retina and choroid is a challenging task due to the formidable obstacles posed by the blood-retinal barrier and the tight junctions of the retinal pigment epithelium. With systemic administration, only small fractions of drug reach the target, requiring large and potentially toxic doses. An ideal method of retinal drug delivery would provide a locally sustained release for prolonged periods of time. Due to the short vitreous half-life of most injectable intravitreal drugs, frequent administrations are necessary. Intravitreal injection has become standard in clinical practice and trials; however,

Correspondence to: Dr L Cheng, Jacobs Retina, Center at Shiley Eye Center, UCSD, 9415 Campus Point, Drive, La Jolla, CA 92037-0946, USA; cheng@eyecenter.ucsd.edu.

Competing interests: UCSD has filed a provisional patent for this intraocular drug-delivery system.

the reported risk of infections is up to 1%, which could lead to devastating visual loss.¹ Intraocular implants have provided sustained vitreoretinal drug levels for treating certain retinal diseases; however, this route demands intraocular surgery that is known to cause complications when placing and replacing the implant.²

We have investigated self-assembling liposomes and, most recently, a crystalline drug-delivery material to achieve intraocular long-lasting release of selected antiviral and antiproliferative compounds.^{3,4} In particular, the lipid prodrug-delivery system is not feasible for delivery of large molecular compounds such as polypeptides and proteins, which are becoming increasingly important in the treatment of eye diseases. Other systems consisting of biodegradable and bioerodible polymeric microparticles have been used to deliver drugs to the posterior segment of experimental animal eyes with a certain degree of success. Many of these particulate systems have been investigated for intraocular drug delivery, but none have demonstrated the capability to provide a non-invasive method to monitor drug release *in vivo*. It is desirable for a drug-delivery system to be capable of housing many types of therapeutics, to be biodegradable after injection, to provide controllable drug release and to allow postinjection monitoring of drug release with a simple optical device in a clinic.

The optical properties of porous Si have been investigated for numerous applications including chemical⁵ and biological⁶ sensors. Porous Si is a biocompatible and bioresorbable material that has also been investigated for *in vivo* drug delivery and biomedical device applications.^{7,8} Recently, we have developed a technique to produce micro particulate photonic crystals from porous Si.⁹ The distinctive particle spectrum can be observed through human tissue,¹⁰ and it can be used to monitor the loading and release of various organic or biomolecules including dexamethasone,¹¹ DNA¹² and bovine serum albumin.¹³ We believe that this optical method of monitoring molecular loading and release is well suited for ophthalmic applications. The drug can be housed in the porous matrix, while the optical spectrum allows non-invasive measurement of the release rate. This is the first study to characterise the intraocular properties of porous silicon particles that are capable of acting as a self-reporting drug-delivery system in living animal eyes.

MATERIALS AND METHODS

Fabrication of porous silicon particles

Porous silicon particles were fabricated by an electrochemical etch of single-crystalline, degenerately B-doped p-type silicon (Siltronix, <100> orientation, $\sim 1 \text{ m}\Omega\cdot\text{cm}$ resistivity) in a 48% aqueous HF:ethanol (3:1 by volume) electrolyte solution. An optical rugate structure was electrochemically etched into the Si wafer using a sinusoidal current modulation of 15-45 mA/cm², with 70 repeats and a periodicity of 12.5 s. The films were removed from the bulk silicon substrate by electropolishing in a 3.3% HF in ethanol solution using a current density of 200 mA/cm² for 2 min. The manufactured porous Si film was generally 20 μm thick (fig 1) with a porosity of 67%, as determined by gravimetric analysis described previously.¹⁴ The freestanding films were then ultrasonically fractured using an ultrasonic cleaner (5 min) to produce particles ranging in size from 1 to 270 μm with over 70% particles falling in the range of 15-30 μm (estimated by optical microscopy). For a 20 μm particle, there is an estimated free volume of $4 \times 10^{-9} \text{ cm}^3$ available for drug loading per particle, with a total free volume of $1.2 \times 10^{-4} \text{ cm}^3$ per particle injection in the rabbit vitreous.

Chemical modification of porous Si particles

Unmodified porous silicon is known to be unstable in aqueous media because of rapid oxidation of the reactive hydride species present on the surface.¹⁵ In this work, two different chemical modification reactions were attempted in order to stabilise the particles. The first method

involves surface alkylation by means of thermal hydrosilylation with 1-dodecene, and the second method is thermal oxidation.^{16,17}

Surface alkylation of porous Si particles

Thermal hydrosilylation was carried out on porous Si particles immediately after their preparation, following the method of Buriak.¹⁶ The particles were placed in a Schlenk flask containing 1-dodecene, and three freeze-pump-thaw cycles were performed to remove oxygen. The reaction flask was filled with nitrogen, and the mixture was heated at 120°C for 2 h. The particles were rinsed thoroughly with dichloromethane and ethanol and then dried in air. The product was characterised by FTIR, confirming the presence of alkyl species on the surface of the particles.

Thermal oxidation of porous Si particles

Oxidation was carried out on porous Si particles immediately after their preparation. Type A: Oxidation was accomplished by heating at 220°C in an oven in ambient air for 24 h. Type B: Oxidation was accomplished by heating at 800°C for 1.5 h in a ceramic dish. Transparency is noticed after oxidation. With highly oxidised films, it was found that sonication does not effectively break the particles into a small enough size regime for injection. Mechanical grinding of the films into particles was used to fracture particles to the desired size instead of ultrasonic fracturing. Most particles are 10-30 µm for injection.

Animal studies

Fourteen New Zealand Red rabbits were used to study the safety and stability of the porous silicon particles in the rabbit vitreous. All of the animal handlings were carried out in adherence to the ARVO Statement for the Use of Animals in Ophthalmic and Vision Research. Using injection methods previously published, one eye of each animal was injected with the porous Si particles, and the fellow eye was injected with the same volume of 5% dextrose to serve as the control.¹⁸ Three rabbits were injected with fresh (not chemically modified) porous Si particles, five rabbits were injected with hydrosilylated porous Si particles, and six were used to evaluate the oxidised porous Si particles (three rabbits for type A and the three others for type B). The particles were suspended in ethanol for sterilisation. Prior to injection, the ethanol was evaporated, and 1 mL of aqueous 5% dextrose solution was added to ~120 mg of the particles. One drop (~6 µL) of sample was taken for particle sizing and counting by light microscopy (fig 2A,B).

A 25-gauge needle was used to deliver 100 µL of the suspension (roughly 12 mg particles) into the rabbit vitreous through the pars plana under direct view of a surgical microscope. After intravitreal injection, the eyes were monitored with an indirect ophthalmoscope, tonometer and biomicroscopic slit-lamp on day 3 and once each subsequent week thereafter.^{18,19} Fundus photography was carried out in the selected rabbit eyes at different intervals after injection to assess degradation of the porous Si particles. The electroretinogram (ERG) was recorded from all eyes of the animals prior to animal sacrifice, which has been described previously.³ After animal sacrifice, the eye globes were enucleated for histology evaluation. The vitreous containing the hydrosilylated porous Si particles was excised from selected eyes, and the particles were examined by scanning electron microscopy.

RESULTS

Observation of unmodified porous Si particles in the rabbit eye

A 100 µL aliquot of porous Si particles in 5% dextrose solution was injected into the vitreous of three eyes of three rabbits using a 25-gauge needle. The particles ranged in size from 1 to

270 μm and the estimated number of particles per injection was approximately 12 000. The particles were suspended in the vitreous at the injection site (fig 3A) and observed to disperse into the surrounding vitreous during the following 2-3 days (fig 3B). During the course of observation, no aqueous flare or cell or decrease in lens or vitreous clarity was noted, and intraocular pressures as well as clinical examination of fundus were normal. The particles degraded completely in 3-4 weeks (fig 3C). Pathological examination by light microscopy revealed normal morphology and structures of retina and choroid without signs of inflammation or retinal cell swelling or loss. No lens damage or iris or ciliary body inflammation was noted (fig 3D).

Observation of hydrosilylated porous Si particles in the rabbit eye

A 100 μL aliquot of hydrosilylated porous Si particles in 5% dextrose solution was injected into the vitreous of five eyes of five rabbits using a 25-gauge needle. The particles ranged in size from 1 to 300 μm (longest dimension) with an estimated 1900 particles per injection. The hydrosilylated particles became distributed throughout the vitreous within 2-3 days while displaying a vivid green colour. Degradation was observed to be much slower than for the unmodified porous Si particles (fig 4A,B). Four months after injection, the animals were sacrificed, and the particles were analysed by optical and by scanning electron microscopy. Approximately 50% of the viewable particles appeared blue-green in colour (fig 4C). The scanning electron microscope images revealed sharp edges on the particles but a pitted surface, indicating some degree of erosion (fig 4D). The other three rabbits were sacrificed for histopathology. ERG examination and tonometry examination were normal, as shown in tables 1, 2; and histology did not show swelling of retinal cells or inflammatory cell infiltration of iris or ciliary body, lens, vitreous, retina or choroid (tables 1, 2).

Observation of oxidised porous silicon particles in the rabbit eye

Type A: A 100 μL aliquot of oxidised porous Si particles in 5% dextrose solution was injected into the vitreous of three eyes of three rabbits using a 25-gauge needle. The particles ranged from 10 to 40 μm , and an estimated 30 000 particles were injected. The oxidised particles showed similar dispersion in the vitreous as the unmodified and the hydrosilylated particles. Faster degradation rates were observed for the oxidised particles than for the hydrosilylated particles (table 1). Two weeks after injection, 20% of the particles showed evidence of degradation, and roughly 80% of them were reflecting purple light (fig 5A,B). Nine weeks after injection, over 80% of the observable particles lost their vivid reflective property and appeared degraded and brown. The particles had settled into the inferior vitreous or retina (fig 5C). The ERG and tonometry examinations were normal (tables 1, 2); and histology showed no inflammatory infiltration of anterior segment, no vitritis and no retinal cell damage or cell loss as compared with the normal control eyes (fig 5D).

Type B: The particles were almost transparent. The size range was 10-30 μm , and the estimated number of particles injected was similar to the type A. The particles initially looked whitish in the vitreous, then degraded to yellowish (fig 6A,B). The estimated half-life was about 2 months. However, the particles were still visible in two of three eyes 12 months after injection (fig 6C), and histology demonstrated normal chorioretinal morphology and structures (fig 6D). The clinical follow-up examination and ERG examination at 16, 24 and 52 weeks were normal (tables 1, 2).

DISCUSSION

The present studies demonstrate that porous Si particles can be safely injected into rabbit vitreous, and the unmodified particles degrade in 3-4 weeks without evidence of toxicity. Chemical modification of the particle and pore surface, either by grafting of dodecyl species

(hydrosilylation) or by conversion to SiO₂ (thermal oxidation), dramatically increases the stability and vitreous residence time of the particles. This suggests that it is plausible for hydrosilylated or oxidised porous Si particles to be used as a long-lasting intravitreal drug-delivery vehicle. Furthermore, by controlling the extent of oxidation or hydrosilylation, we suggest the vitreous residence time of the particles can be manipulated to fit the specific treatment modality.

Porous Si has been studied previously in physiological aqueous solutions and was found to dissolve into the form of orthosilicic acid, which is vital for normal bone and connective tissue homeostasis.²⁰ However, porous Si dissolution has never been studied in vitreous, which is a complex biological solution with constant fluid turn over. This type of condition is not easily duplicated in an in vitro setting. Therefore, the dissolution and the associated potential toxicity must be studied directly in living eyes.

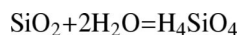
The unique photonic properties of porous Si make this material ideal for drug delivery by imparting a potential self-reporting feature within the delivery system. The wavelength of the spectral peak reflected from porous Si photonic crystals is dependent on the refractive index (n) of the porous Si matrix.²¹ Changes in the refractive index of the porous Si layer occur as aqueous solution (n = 1.34) replaces organic molecules or proteins (n~1.4) in the pores, resulting in a blue shift of the reflectivity peak and an observable colour change.²² A spectral blue shift is also expected as the Si matrix (n~3.5) is oxidised to SiO₂ (n~1.7) or as the SiO₂ matrix dissolves. In the present case, the initial green colour of the photonic crystals is observed to turn blue or violet after several days to weeks in vitreous (depending on the surface chemistry) indicating dissolution of the porous matrix. After extended periods in vitreous, some of the particles lose their vivid reflectance and appear brown in colour. The brown colour is attributed to light absorption by residual Si in a particle whose photonic signature has shifted into the ultraviolet range. It is also possible that the signature spectrum of the photonic crystal no longer exists due to extensive degradation of the periodic nanostructure. This unique signature spectrum of the photonic crystal could be utilised to monitor drug release through the transparent optical medium of the eye using a simple CCD spectrometer device that would provide a non-invasive method to monitor drug release. This would be a major advantage over other drug-delivery materials such as biodegradable and bioerodible polymeric microparticles.

It is possible that the injected particles could interfere with vision initially. However, with dispersion and settling of the particles into the inferior vitreous cavity, the possibility of interference will diminish. In clinical practice, many patients who have asteroid hyalosis seem to not be aware of the presence of the vitreous crystals.²³

The fact that certain preparations of the porous Si particles have long vitreous lifetimes and display no apparent toxicity supports the feasibility of the use of porous Si as an intravitreal delivery material. With the advent of many intravitreal injectable therapeutics, such as dexamethasone, pegaptanib (Macugen), bevacizumab (Avastin) and the recently FDA-approved ranibizumab (Lucentis), repeated intravitreal injections can potentially generate serious problems. These procedures impose life-quality issues with patients and raise the risk of intraocular infections. If the drugs could be trapped in porous Si microparticles by some encapsulant or by covalent or electrostatic interactions between the drug and the porous Si particles, then the drug would be slowly released as the particles degrade. This would eliminate the necessity of frequent injections.

A 100 µl intravitreal injection as used in our rabbit studies typically contains ~30 000 porous Si particles, each approximately 50 µm square and 20 µm thick. We estimate that we can load at least ~50 mg of dexamethasone per gram of porous Si material.¹¹ If we assume that the porous Si particles display first-order dissolution kinetics and that drug release occurs

concomitant with particle dissolution, then the steady-state concentration of drug in the eye can be approximated using the dissolution mechanisms of Dove and Craven.²⁴ With this model, the dissolution of the porous Si particles can be approximated by this overall reaction:²⁵



where the species H_4SiO_4 represents the water-soluble forms of silicic acid (at various stages of protonation and oligomerisation). The rate expression for this reaction is dependent on the total surface area of the particles exposed to solution and the mass flow rate of silicic acid out of the system. For the present particulate system, we assume that the appearance of silicic acid in solution will correlate with the appearance of drug in solution. This upper estimate is expected to hold if, for example, the drug is covalently attached to the porous Si matrix via the surface hydrosilylation reaction. As the particles dissolve, the drug would be released, and the steady-state concentration of drug in the eye can be calculated based on the following relationship that has been adapted from Dove's model (assuming that the total surface area of particles exposed to solution is proportional to the number of particles, N):

$$M_d = [t_{1/2}(\text{drug}) / t_{1/2}(\text{particle})] \times N \times L$$

where M_d is the mass of free drug in the vitreous, N is the number of particles injected per eye, L is the mass of drug loaded per particle, $t_{1/2}(\text{drug})$ is the half-life of free drug in vitreous, and $t_{1/2}(\text{particle})$ is the half-life of the particles in vitreous.

We assume that the longer the particle half-life, as demonstrated for the hydrosilylated particles and oxidised particles, the lower the steady-state concentration of drug. For particles with a 60-day half-life and an initial loaded drug mass of 600 μg in 12 mg of porous Si particles ($\sim 30\,000$ particles), the steady-state concentration of dexamethasone with a vitreous half-life of 3.48 h²⁶ would be $\sim 1\ \mu\text{g}/\text{mL}$ in rabbit vitreous (1.4 ml), which is above the therapeutically relevant dose of $>5\ \text{ng}/\text{mL}$.²⁷ We expect the particles to deliver drug at therapeutically relevant quantities for at least two half-lives of the particles (120 days).

Drugs with a longer vitreous half-life such as Avastin (5 days) should be able to further extend the period between injections. For Avastin, we estimate a loading capacity of 20 mg of drug per gram of particles. Thus, the initial amount of drug in a 0.1 cm^3 injection of porous Si loaded with Avastin would be 240 μg of drug. If the half-life of the particles is 60 days, the steady-state concentration of drug in vitreous would be $\sim 14\ \mu\text{g}/\text{mL}$. The therapeutically relevant dose of Avastin as an intraocular treatment is generally considered to be $>22\ \text{ng}/\text{mL}$.²⁸

In summary, the current study demonstrates the intravitreal biocompatibility of porous Si microparticles and the feasibility of porous Si as a platform for an intraocular drug-delivery system. Further studies to characterise the drug loading, intravitreal release profiles, and non-invasive remote monitoring of drug release are needed to determine the viability of the approach for effective patient treatment.

Acknowledgements

Funding: (1) Unrestricted research fund to Jacobs Retina Center, UCSD (Freeman & Cheng). (2) Supported in part by Research to Prevent Blindness (Freeman). (3) National Science Foundation, Grant# DMR-0503006 (MJS). MJS is a member of the Moores UCSD Cancer Center and the UCSD NanoTUMOR Center under which this research was conducted and partially supported by NIH grant U54 CA 119335. The CNRS/DREI program (call for proposal CNRS/United States 2005 #3312) is also acknowledged for financial support.

REFERENCES

1. D'Amico DJ, Bird AC. VEGF Inhibition study in ocular neovascularization-1 (VISION-1): safety evaluation from the pivotal Macugen™ (pegaptanib sodium) clinical trials [E-abstract]. *Invest Ophthalmol Vis Sci* 2004;45:2363.
2. Martin DF, Ferris FL, Parks DJ, et al. Ganciclovir implant exchange. Timing, surgical procedure, and complications. *Arch Ophthalmol* 1997;115:1389–94. [PubMed: 9366668]
3. Cheng L, Hostetler KY, Chaidhawangul S, et al. Treatment or prevention of herpes simplex virus retinitis with intravitreally injectable crystalline 1-*O*-hexadecylpropanediol-3-phospho-ganciclovir. *Invest Ophthalmol Vis Sci* 2002;43:515–21. [PubMed: 11818399]
4. Cheng L, Hostetler KY, Lee J, et al. Characterization of a novel intraocular drug delivery system using crystalline lipid antiviral prodrugs of ganciclovir and cyclic cidofovir. *Invest Ophthalmol Vis Sci* 2004;45:4138–44. [PubMed: 15505067]
5. Sailor, MJ.; Trogler, WC.; Content, S., et al. In: Carapezza, EM.; Law, DB.; Stalker, KT., editors. Detection of DNT, TNT, HF and nerve agents using photoluminescence and interferometry from a porous silicon chip; SPIE Meeting on Unattended Ground Sensor Technologies and Applications; Orlando, FL: SPIE. 2000;
6. Dancil, K-PS.; Greiner, DP.; Sailor, MJ. In: Canham, LT.; Sailor, MJ.; Tanaka, K.; Tsai, C-C., editors. Development of a porous silicon based biosensor; Materials Research Society Symposium Proceedings; Boston. 1999;
7. Porter AE, Buckland T, Hing K, et al. The structure of the bond between bone and porous silicon-substituted hydroxyapatite bioceramic implants. *J Biomed Mater Res A* 2006;78:25–33. [PubMed: 16596583]
8. Radin S, El-Bassyouni G, Vresilovic EJ, et al. In vivo tissue response to resorbable silica xerogels as controlled-release materials. *Biomaterials* 2005;26:1043–52. [PubMed: 15369693]
9. Cunin F, Schmedake TA, Link JR, et al. Biomolecular screening with encoded porous silicon photonic crystals. *Nat Mater* 2002;1:39–41. [PubMed: 12618846]
10. Li YY, Cunin F, Link JR, et al. Polymer replicas of photonic porous silicon for sensing and drug delivery applications. *Science* 2003;299:2045–7. [PubMed: 12663921]
11. Anglin EJ, Schwartz MP, Ng VP, et al. Engineering the chemistry and nanostructure of porous silicon Fabry-Pérot films for loading and release of a steroid. *Langmuir* 2004;20:11264–9. [PubMed: 15568884]
12. Lin VS, Motesharei K, Dancil KP, et al. A porous silicon-based optical interferometric biosensor. *Science* 1997;278:840–3. [PubMed: 9346478]
13. Collins BE, Dancil KPS, Abbi G, et al. Determining protein size using an electrochemically machined pore gradient in silicon. *Advanced Functional Materials* 2002;12:187–91.
14. Halimaoui, A. Porous silicon formation by anodisation. In: Canham, L., editor. Properties of porous silicon. Vol. 18. Short Run Press; London: 1997.
15. Lees IN, Lin H, Canaria CA, et al. Chemical stability of porous silicon surfaces electrochemically modified with functional alkyl species. *Langmuir* 2003;19:9812–17.
16. Buriak JM. Organometallic chemistry on silicon and germanium surfaces. *Chem Rev* 2002;102:1272–308.
17. Boukherroub R, Wayner DDM, Sproule GI, et al. Stability enhancement of partially-oxidized porous silicon nanostructures modified with ethyl undecylenate. *Nano Lett* 2001;1:713–17.
18. Cheng L, Hostetler KY, Gardner MF, et al. Intravitreal toxicology in rabbits of two preparations of 1-*O*-octadecyl-sn-glycerol-3-phosphonoformate, a sustained-delivery anti-CMV drug. *Invest Ophthalmol Vis Sci* 1999;40:1487–95. [PubMed: 10359331]
19. Cheng L, Hostetler KY, Lee J, et al. Characterization of a novel intraocular drug-delivery system using crystalline lipid antiviral prodrugs of ganciclovir and cyclic cidofovir. *Invest Ophthalmol Vis Sci* 2004;45:4138–44. [PubMed: 15505067]
20. Anderson SHC, Elliott H, Wallis DJ, et al. Dissolution of different forms of partially porous silicon wafers under simulated physiological conditions. *Phys Status Solidi A* 2003;197:331–5.
21. Link JR, Sailor MJ. Smart Dust: Self-assembling, self-orienting photonic crystals of porous Si. *Proc Natl Acad Sci* 2003;100:10607–10. [PubMed: 12947036]

22. Sailor MJ, Link JR. Smart Dust: nanostructured devices in a grain of sand. *Chem Commun* 2005;1375–83.
23. Hwang JC, Barile GR, Schiff WM, et al. Optical coherence tomography in asteroid hyalosis. *Retina* 2006;26:661–5. [PubMed: 16829809]
24. Dove PM, Craven CM. Surface charge density on silica in alkali and alkaline earth chloride electrolyte solutions. *Geochim Cosmochim Acta* 2005;69:4963–70.
25. Dove PM, Crerar DA. Kinetics of quartz dissolution in electrolyte-solutions using a hydrothermal mixed flow reactor. *Geochim Cosmochim Acta* 1990;54:955–69.
26. Kwak HW, Damico DJ. Evaluation of the retinal toxicity and pharmacokinetics of dexamethasone after intravitreal injection. *Arch Ophthalmol* 1992;110:259–66. [PubMed: 1736876]
27. Weijtens O, Schoemaker RC, Cohen AF, et al. Dexamethasone concentration in vitreous and serum after oral administration. *Am J Ophthalmol* 1998;125:673–9. [PubMed: 9625551]
28. Wang Y, Fei D, Vanderlaan M, et al. Biological activity of bevacizumab, a humanized anti-VEGF antibody in vitro. *Angiogenesis* 2004;7:335–45. [PubMed: 15886877]

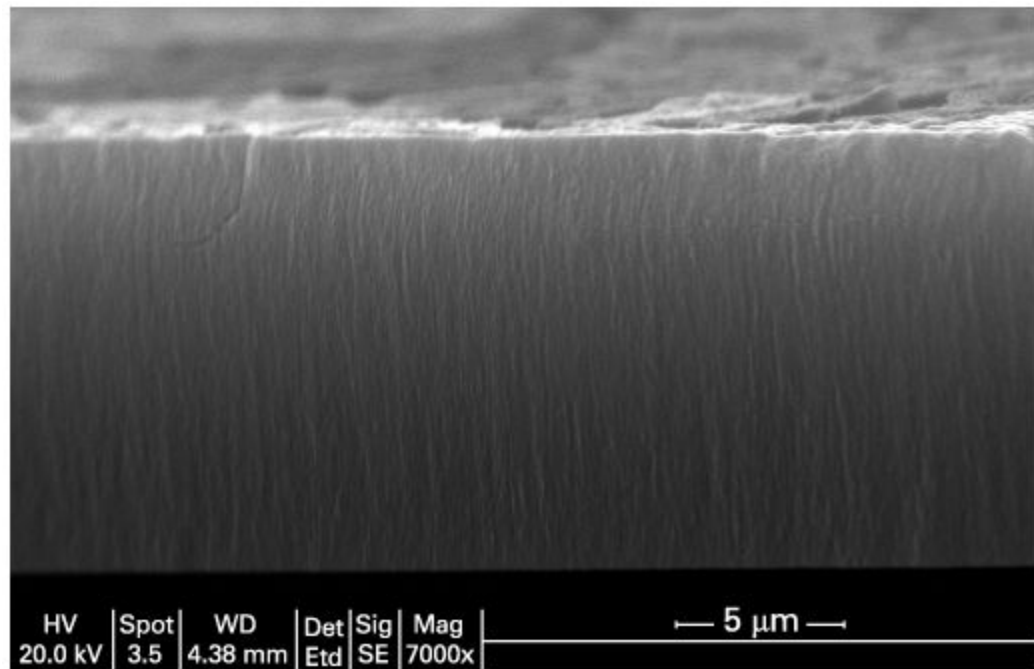


Figure 1.

Cross-sectional scanning electron micrograph image of an intact porous Si film prior to removal from the bulk silicon substrate and fracture into microparticles. The pores are aligned along the $\langle 100 \rangle$ direction of the original silicon crystal.

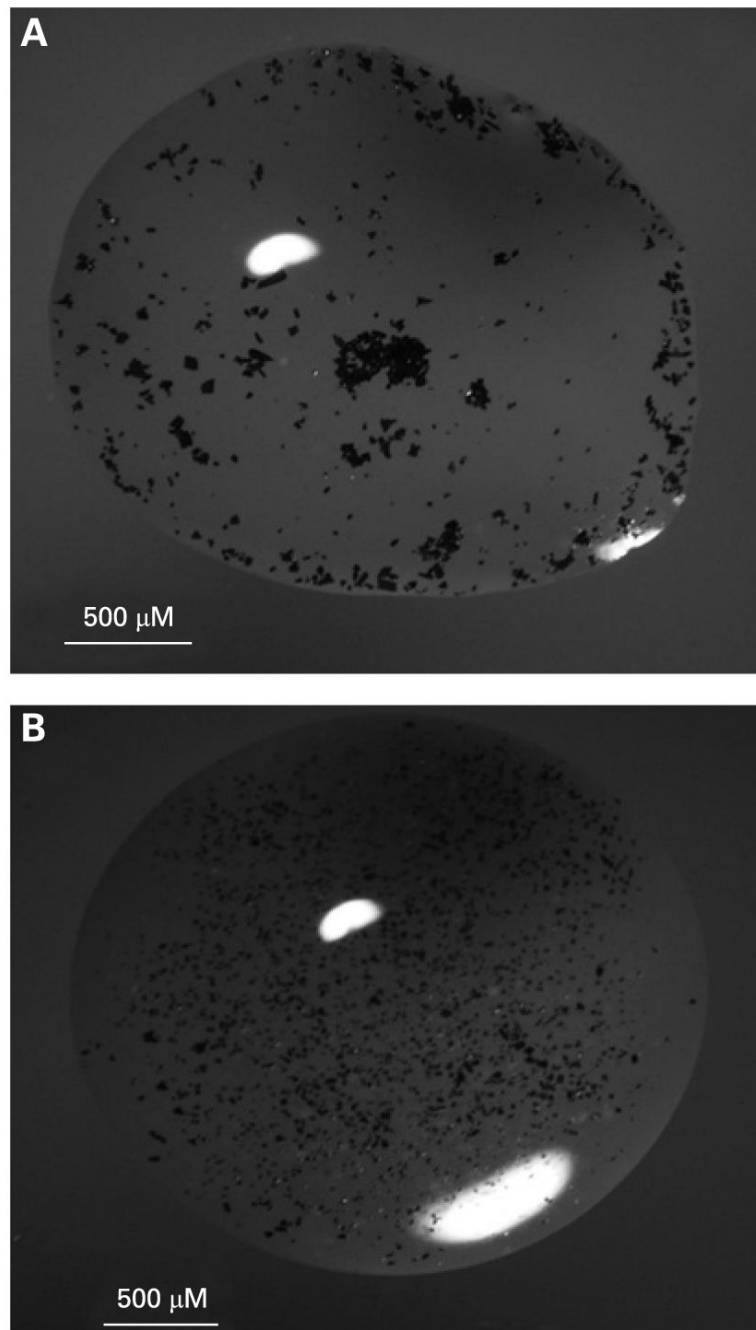


Figure 2. (A) Fresh porous Si particles in a droplet of 5% dextrose solution. Particle clumping is observed due to the hydrophobic nature of the unmodified porous Si particles. (B) Oxidised particles in a droplet of 5% dextrose solution. These particles were observed to be more dispersed in solution, presumably because of the hydrophilic nature of the SiO₂ surface.

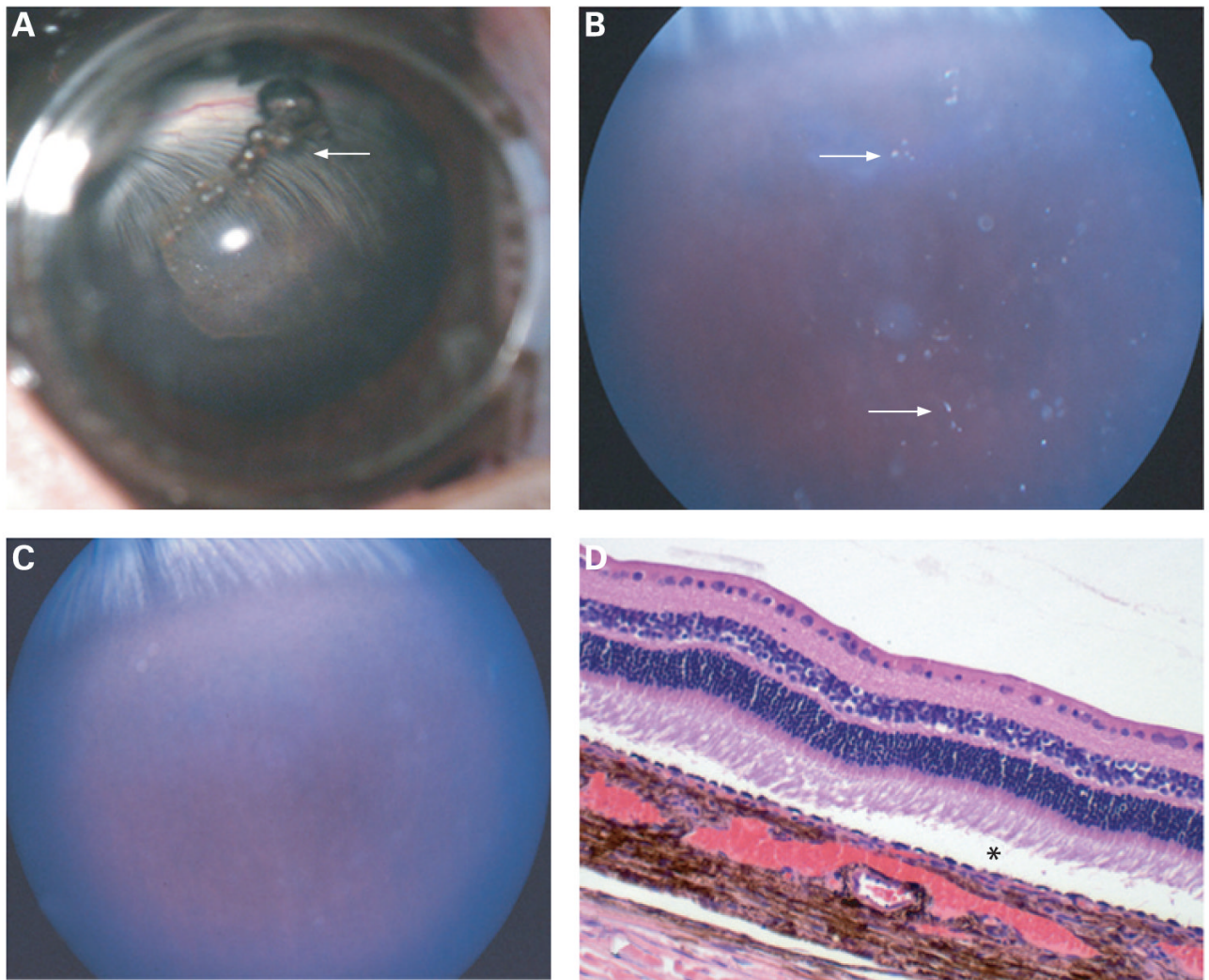


Figure 3.

(A) Photograph taken under a surgical microscope immediately after intravitreal injection of fresh porous Si particles. Particles can be observed suspended in the centre of the vitreous. A few small air bubbles mixed with the porous silicon particles are present at the top of the vitreous cavity (arrow). (B) Fundus photograph taken 1 week after the injection, showing porous Si particles dispersed in the vitreous (arrows). (C) Fundus photograph taken 2 weeks after injection, indicating that most of the particles have disappeared, and those remaining are barely observable. (D) Light microscopic image shows normal retina and choroids with a slight artefact of retinal detachment (asterisk) (33 \times , H&E staining).

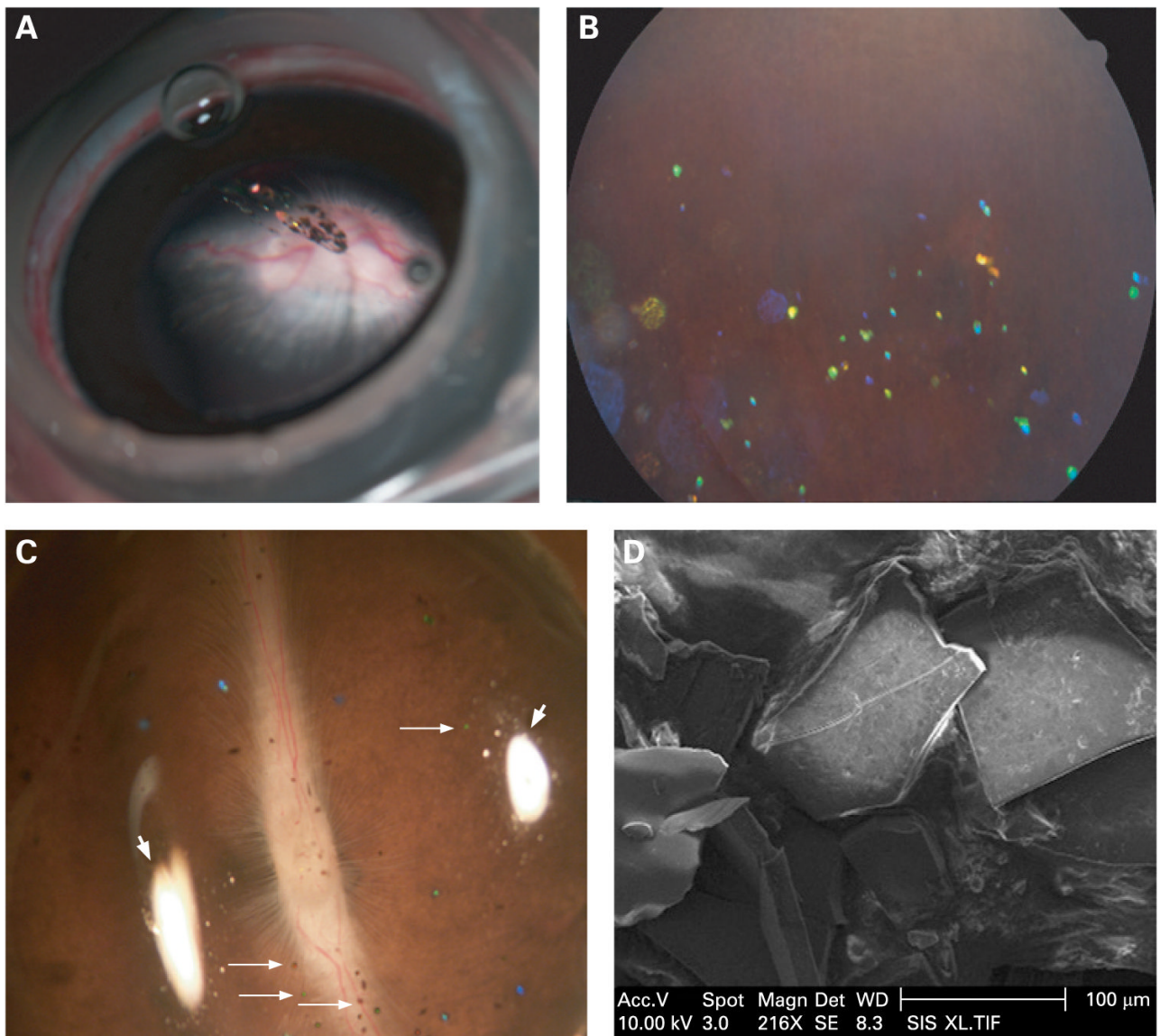


Figure 4.

(A) Photograph taken under a surgical microscope immediately after intravitreal injection of hydroxylated porous Si particles. Particles can be observed suspended in the centre of the vitreous. (B) Fundus photograph obtained 3 months after injection. The particles are dispersed in the vitreous, and many demonstrated a distinctive blue colour corresponding to partial degradation and dissolution. (C) Dissecting microscope image of a rabbit eye cup, with hydroxylated porous Si particles (small arrows) distributed on a normal-looking retina. Photograph was obtained 4 months after injection. Two white areas (large arrows) evident in the image arise from reflections of the illumination source. (D) Scanning electron microscope image of the hydroxylated porous Si particles sampled from a rabbit eye 4 months after intravitreal injection. The sharp edges and pitted surface of the particles indicate a very slow erosion process.

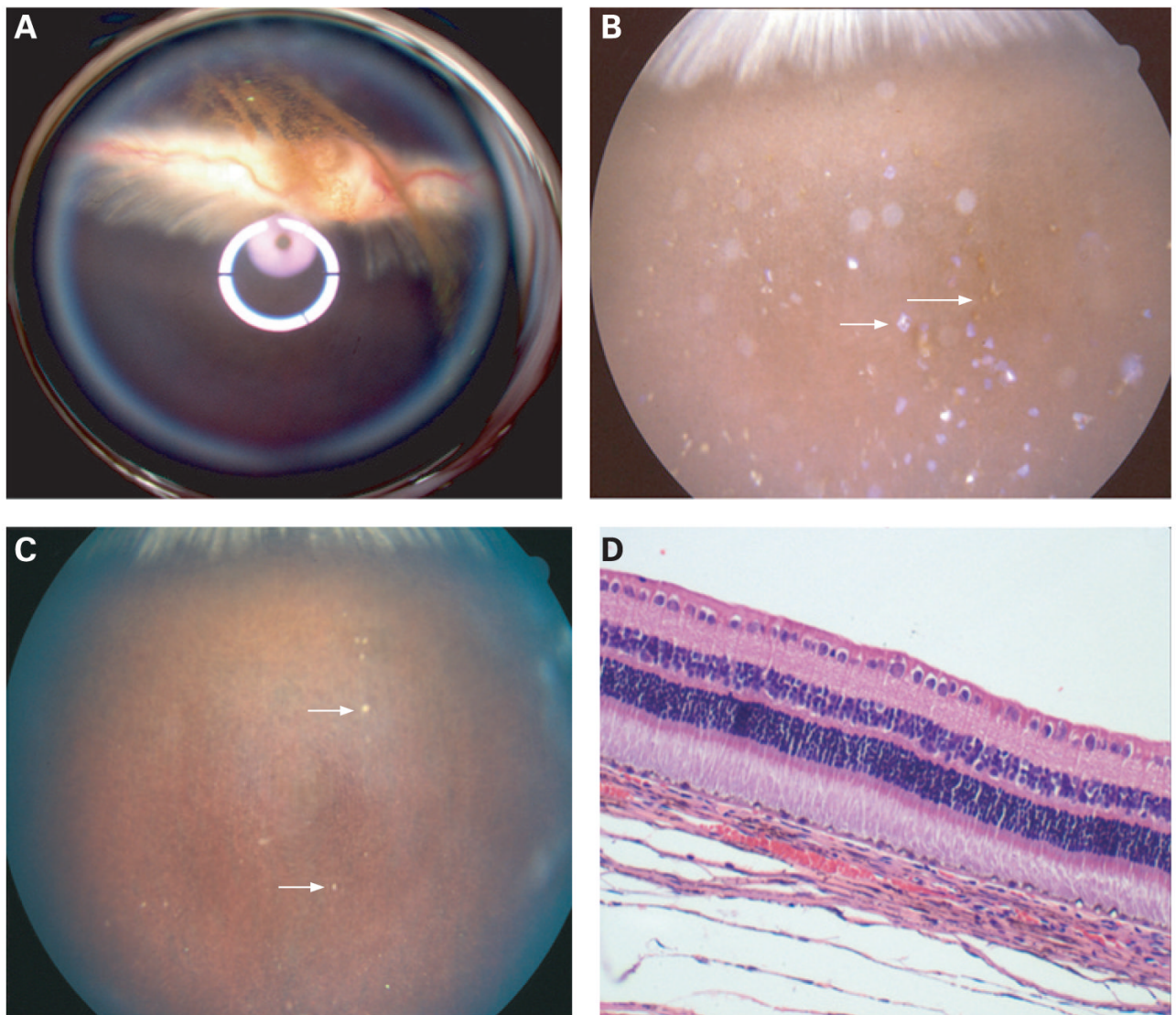


Figure 5.

(A) Fundus photograph taken immediately after intravitreal injection of oxidised porous Si particles using a Volk Pan retinal 2.2 lens coupled to the Canon fundus camera lens for a wider view of the fundus. The white and purple rings were from the lens reflection. Particles can be observed suspended in the centre of the vitreous above the optic nerve. (B) Fundus photograph of a rabbit eye 2 weeks after intravitreal injection of oxidised porous Si particles. Many violet (small arrow) particles can be seen. The violet colour indicates that significant oxidation and dissolution of the particles have occurred. Some of the particles have lost their vivid reflectance completely and appear brown in colour (large arrow). (C) Fundus photograph of the same rabbit eye, 9 weeks after intravitreal injection of oxidised porous Si particles. Many of the particles have degraded, and only a few brownish particles are observed (arrows). The fundus appears normal. (D) Light microscopic photograph of the retina and choroid from a rabbit eye harvested 4 months after intravitreal injection of oxidised porous Si particles. Normal chorioretinal morphology and structures are observed (33 \times , H&E staining).

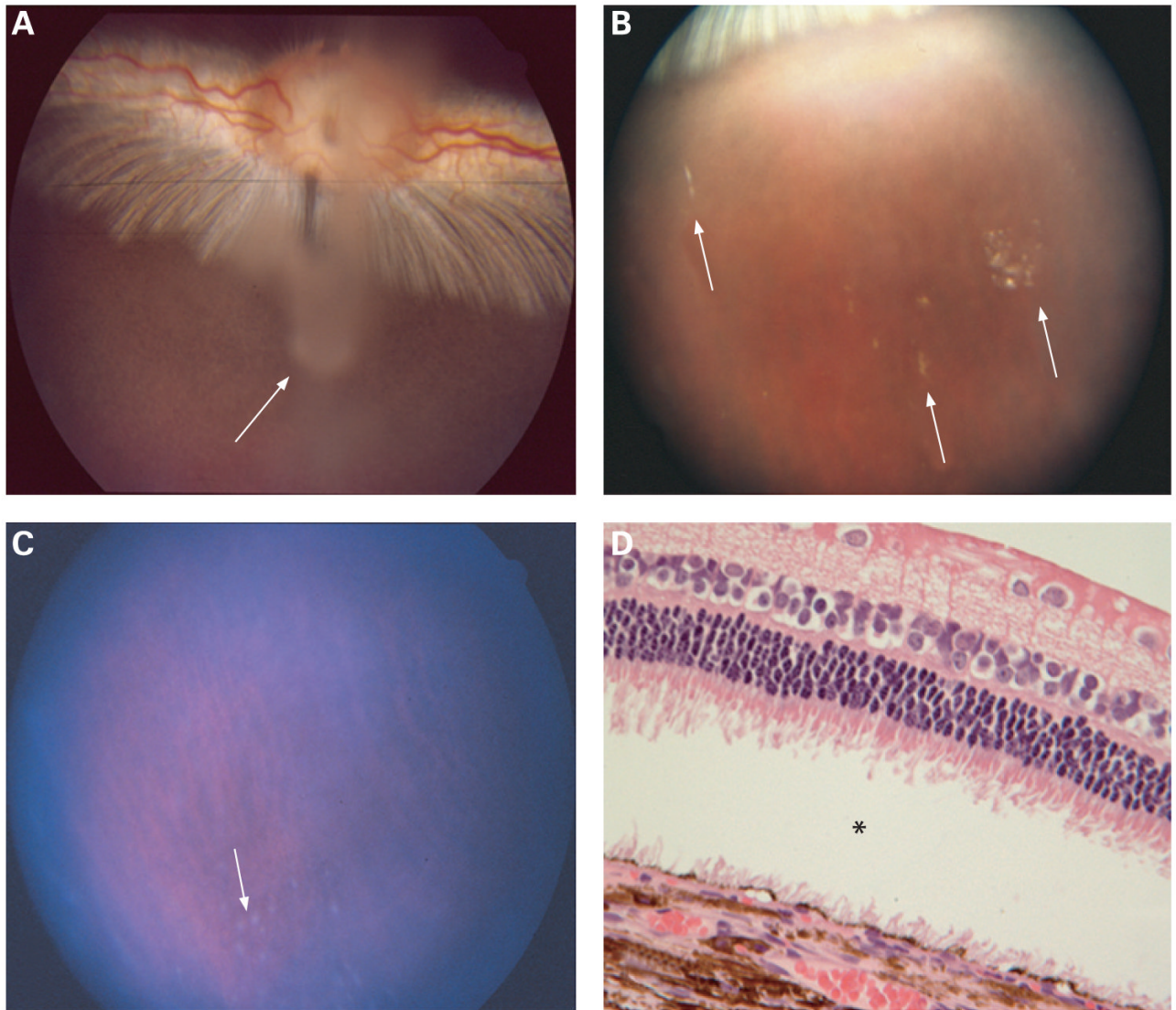


Figure 6.

(A) Fundus photograph taken 3 days after intravitreal injection of type B oxidised porous Si particles. Whitish aggregates of the particles can be observed suspended in the centre of the vitreous above the optic nerve (arrow). (B) Fundus photograph of a rabbit eye 2 months after intravitreal injection. The particles are dispersed, with a yellowish appearance (arrows). (C) Fundus photograph of a rabbit eye 5 months after intravitreal injection. Many of the particles have degraded; however, some greyish particles are still observed in the very inferior vitreous (arrow). (D) Light-microscopic photograph of the retina and choroid from a rabbit eye harvested 8 months after intravitreal injection. Normal chorioretinal morphology and structures are observed except for the artificial retinal detachment (asterisk) (62.5 \times , H&E staining).

Table 1
Characterisation of the different types of porous silicon particles after intravitreal injection

Particle type	No. of eyes tested	Maximum vitreous residence time	Estimated vitreous half-life by ophthalmoscopy	Bio-microscopy* and indirect ophthalmoscopy	Intraocular pressure	Electroretinography	Pathology
Unmodified (fresh)	3	4 weeks	1 week	Normal at all checking points	Normal at 1, 2, 4 weeks	Normal at 4 weeks	Normal at 4 weeks
5% dextrose	3	NA	NA	Normal at all checking points	Normal at 1, 2, 4 weeks	Normal at 4 weeks	Normal at 4 weeks
Hydrosilylated	5	.17 weeks	16 weeks	Normal at all checking points	Normal at 1, 2, 4, 12, 17 weeks	Normal at 12, 17 weeks	Normal at 17 weeks
5% dextrose	5	NA	NA	Normal at all checking points	Normal at 1, 2, 4, 12, 17 weeks	Normal at 12, 17 weeks	Normal at 17 weeks
Oxidised	3	12 to .18 weeks	5 weeks	Normal at all checking points	Normal at 1, 2, 4, 12, 18 weeks	Normal at 12, 18 weeks	Normal at 18 weeks
5% dextrose	3	NA	NA	Normal at all checking points	Normal at 1, 2, 4, 12, 18 weeks	Normal at 12, 18 weeks	Normal at 18 weeks
Oxidised at high temperature	3	10 to 12 months	8 weeks	Normal at all checking points	Normal at 2, 6, 16, 24, 40, 52 weeks	Normal at 16, 24, 40, 52 weeks	Normal at 12 months
5% dextrose	3	NA	NA	Normal at all checking points	Normal at 2, 6, 16, 24, 40, 52 weeks	Normal at 16, 24, 40, 52 weeks	Normal at 12 months

* Slit-lamp examination of cornea, anterior chamber, lens, vitreous, and indirect ophthalmoscopy of fundus.

Results of intraocular pressure and electroretinography from eyes with the different types of porous silicon particles (or 5% dextrose control)

Table 2

Particle type	No. of eyes tested	Intraocular pressure (mm Hg)	Electroretinography a-wave implicit (mS)	Electroretinography a-wave amplitude (μV)	Electroretinography b-wave implicit (mS)	Electroretinography b-wave amplitude (μV) [†]
Unmodified (fresh)	3 (OD)	18.7 (4) (at week 4)	16 (0)	20.3 (0.6)	71.3 (4.2)	70 (12)
5% dextrose	3 (OS)	15.7 (2) (at week 4)	16 (0)	20 (0)	71.3 (4.2)	85 (27)
Hydroxylated	5 (OD)	18.2 (2) (at week 17)	12.3 (1.1)	31.3 (5.1)	67.3 (6.8)	143 (31.6)
5% dextrose	5 (OS)	19 (2) (at week 17)	12.3 (1.1)	27 (2)	67.7 (6.8)	142.3 (18.8)
Oxidised	3 (OD)	9 (1) (at week 18)	14 (1.7)	18.6 (1.2)	70.7 (9.2)	86.7 (24.7)
5% dextrose	3 (OS)	9 (1) (at week 18)	14 (1.7)	19.3 (1.1)	70.7 (9.2)	71.7 (15.9)
Oxidised at high temperature	3 (OD)	15.3 (2) (at 12 months)	21.3 (2.3)	18.5 (1.5)	71.7 (10.4)	83.7 (27)
5% dextrose	3 (OS)	15.7 (2) (at 12 months)	21.3 (2.3)	18.8 (1)	65 (10)	91.3 (32.5)

OD, right eye; OS, left eye.

* Intraocular pressure was statistically analysed by paired t test (OD vs OS), $p = 0.71$.

[†] b-Wave amplitude was statistically compared between OD and OS using a paired t test ($p = 0.77$).